31-Phosphorus Magnetic Resonance Spectroscopy in Evaluation of Glioma and Metastases in 3T MRI

S. Babu Peter[1] V. Raghu Nandhan[1]

[1] Department of Radiodiagnosis, Barnard Institute of Radiology, Madras Medical College, Chennai, Tamil Nadu, India

Indian J Radiol Imaging 2021;31:873–881.

Address for correspondence S. Babu Peter, MDRD, DNB, FICR, Department of Radiodiagnosis, Barnard Institute of Radiology, Madras Medical College, Chennai, Tamil Nadu 600003, India (e-mail: drbabupeter@gmail.com).

Abstract

Background: 31-Phosphorus magnetic resonance spectroscopy (31-P MRS) has excellent potential for clinical neurological practice because of its noninvasive in-vivo assessment of cellular energy metabolism and the indirect evaluation of the phospholipid composition of the cell membrane, intracellular pH, and intracellular Mg2+ concentration.

Purpose: The aim of this study was to evaluate the metabolic characteristics of glioma and metastases using 31-P MRS and assess utility to differentiate both.

Study Type: Prospective study.

Population: Fifteen consecutive patients with brain tumor.

Field Strength/Sequence: Three-tesla magnetic resonance imaging/three-dimensional MRS imaging sequence.

Statistical Tests: Unpaired sample *t*-test, and one-way analysis of variance with Tukey's post-hoc test.

Results: Significantly decreased values of phosphomonoesters/inorganic phosphate (PME/Pi) in the tumor group (1.22 ± 0.72) compared with controls (2.28 ± 1.44) with a *p*-value of 0.041 were observed. There is a significant decrease in phosphocreatine (PCr)/Pi values (energy demand) in the tumor group (2.76 ± 0.73) compared with controls (4.13 ± 1.75) with a *p*-value of 0.050. Significant increase in Pi/adenosine triphosphate (ATP) was noted in tumor group (0.28 ± 0.09) compared with controls (0.22 ± 0.08) with *p*-value 0.049. Among tumor group, PME/PCr values were significantly decreased in gliomas (0.35 ± 0.17) than metastasis (0.58 ± 0.23) compared with controls with a *p*-value of 0.047. A significant decrease in PME/ATP was noted in gliomas (0.25 ± 0.12) than metastasis (0.41 ± 0.14) compared with controls with a *p*-value of 0.034. The tumor group exhibits alkaline pH (7.12 ± 0.10) compared with the normal parenchyma (7.04 ± 0.06) with a significant *p*-value of 0.025. Glioma and metastasis could not be differentiated with pH. However, the perilesional edema of glioma shows alkaline pH (7.09 ± 0.06) and metastasis shows acidic pH (7.02 ± 0.05) with a significant *p*-value of 0.030.

Conclusion: Our study provides new insight into the cellular constituents and pH of gliomas and metastases and results were significant in differentiation between these two. However, due to the additional high expense, it is available as a research tool in very few institutions in India.

Keywords

- nuclear magnetic spectroscopy
- 31-phosphorus multinuclear spectroscopy
- glioma
- metastases

published online
January 10, 2022

DOI https://doi.org/10.1055/s-0041-1741090.
ISSN 0971-3026.

Thieme Medical and Scientific Publishers Pvt. Ltd., A-12, 2nd Floor, Sector 2, Noida-201301 UP, India

Introduction

Nuclear magnetic resonance (NMR) spectroscopy is now an advanced tool for proper elucidation of the chemical structure and chiral recognition. Among the active NMR nuclei, 1H is most frequently used because of its environmental abundance. But it poses certain limitations and to overcome these, newer NMR nuclei like 19F, 31P, 13C, and 77Se have been used. They have larger shift dispersion and are useful for analysis.

There is a potential for 31-phosphorus magnetic resonance spectroscopy (31-P MRS) to be used in clinical neurological practice because of its noninvasive in-vivo assessment of cellular energy metabolism and the indirect evaluation of the phospholipid composition of the cell membrane, intracellular pH, and intracellular Mg2+ concentration. Phosphorus metabolites like phosphocreatine (PCr), inorganic phosphate (Pi), and adenosine triphosphate (ATP) are the key metabolites in cellular energy production.[1] Thus, 31-P MRS helps in the measurement and quantification of these metabolites, assessment of cellular viability and integrity, and also in the estimation of intracellular parameters like pH. However, coarse spatial recognition, long acquisition time, long longitudinal relaxation time (T1 values), short transverse relaxation time (T2), and low signal-to-noise ratio hinder the efficient signal acquisition with high spatial configuration.[2] Ultra-high-frequency scanners and newer coils can overcome these limitations in the coming future. In the brain and skeletal muscle, the dominant signal is from PCr, which is usually assigned a chemical shift of 0 ppm due to its relative stability and prominence. Pi and the phospholipids, including phosphomonoesters (PME) and phosphodiesters (PDE), are located to the left of PCr. Resonant peaks from the three phosphate groups of ATP (γ-, α-, and β-ATP from left to right) are located to the right of PCr[3] (►**Fig. 1**). PCr is used for storing energy and converting adenosine diphosphate (ADP) to ATP. It is absent in the liver, kidney, and red cells. ATP is the energy currency in living systems. β- and γ-ATP have contributions from ADP, nicotinamide adenine dinucleotide, and nicotinamide adenine dinucleotide + hydrogen.[4] β-ATP is uncontaminated and used for quantification. PME signal contains a contribution from membrane constituents and glucose-6-phosphate and glycerol-3 phosphate. PME signal contains a contribution from membrane constituents and it is elevated in tumors.[5] The chemical shifts of many phosphorus compounds are pH-dependent because the protonation of a compound changes the electron distribution surrounding the nuclei and thus changes their resonance frequencies. In a 31-P spectrum, the chemical shift of Pi is most sensitive to changes in pH near neutrality because the dissociation constant (pK) of Pi, that is, the pK, is approximately the ratio of PCr to total-mobile-phosphate (defined as the combined signals PCr plus γATP plus Pi) and the ratio of γ-ATP to total-mobile-phosphate.[6]

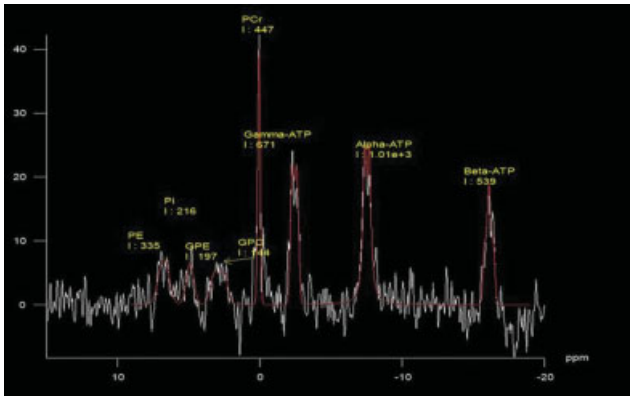

Fig. 1 Spectral waveform of various phospholipid metabolites in normal brain parenchyma.

Aim and Objective

This study aims to evaluate the significance and assess the various metabolites and metabolite ratios in gliomas and intraparenchymal cerebral metastasis using 31-phosphorus multinuclear spectroscopy (31-P MNS) and to calculate the biochemical pH within these tumors and utility to differentiate both.

Inclusion and Exclusion Criteria

Patients who were referred for imaging of brain space occupying lesions (SOL) were included in our study. Postoperative cases that came for follow-up were excluded. Similarly, lesions with extensive gradient blooming due to hemorrhage, occupying more than one-third of voxel, were excluded from the study.

Materials and Methodology

The prospective cross-sectional study was conducted from February 2020 to July 2020 (6 months) after obtaining the approval of the Institutional Ethics Committee. Fifteen ($n = 15$) consecutive patients who were referred to our department for imaging of brain SOL were initially done routine magnetic resonance imaging (MRI) of brain with standard institute protocol and followed by 31-P MNS in 3-tesla MRI (Skyra, Siemens Healthineers, Erlangen, Germany). This was performed using a specially designed double-tuned volume H1/P31 head coil (Rapid Biomedical, Wurzburg, Germany) with both channels equipped with quadrature polarization and with an inner diameter of 26.5 cm and housing length of 43 cm. For 31-P spectroscopy, a three-dimensional MRS imaging sequence with wideband alternating phase encoding low-power technique for zero residual splitting proton decoupling was used with flip angle 90, bandwidth 3,000 Hz, repetition time 1,000 ms, echo time 2.3 ms, 9 acquisition and acquisition time of 15:04 s.[7] After analyzing the routine sequences, postprocessing was done in Siemens workstation, the voxel of interest was selected with an extrapolated $8 \times 8 \times 16$ matrix, and a field of view of $240 \times 240\ mm^2$, resulting in a voxel size of $40.0 \times 40.0 \times 25.0\ mm^3$ and placed in three selected areas:[7] one within the contrast-enhanced tumor area, the other in the peritumoral border (nonenhancing edema), and the final in the

contralateral brain parenchyma. The integral values of PCr, Pi, PME, PDE, and ATP were noted from the three areas of interest. The following ratios were calculated: PME/PDE (membrane turnover), pCr/Pi (energy demand), pCr/ATP (resynthesis), Pi/ATP (hydrolysis), PME/Pi, PME/pCr, PME/ATP, PDE/Pi, PDE/pCr, PDE/ATP, and ATP/Pi. pH values were calculated in the same areas of interest using the following Henderson–Hasselbalch formulae,[8]

$$pH = 6.66 + \log \frac{\delta Pi - 3.08}{5.57 - \delta Pi}$$

$$pH = 6.77 + \log \frac{\delta Pi - 3.29}{5.68 - \delta Pi}$$

where δpi is the difference in chemical shift of Pi and PCr.

The cases were followed-up after surgery for histopathological results and to confirm the diagnosis.

Statistical Analysis

The collected data were analyzed with Statistical Package for the Social Sciences (IBM, Armonk, New York, United States) statistics software 23.0 Version. To describe the data, descriptive statistics frequency analysis was done, percentage analysis was used for categorical variables, and the mean and standard deviation (SD) were used for continuous variables. To find the significant difference between the bivariate samples in independent groups, the unpaired sample *t*-test was used. For the multivariate analysis, the one-way analysis of variance with Tukey's post-hoc test was used. In all the above statistical tools, the probability value of 0.05 is considered as a significant level.

Results

►**Tables 1** and **2** show the mean and SD of integral values of various phospholipid metabolites, and various ratios with statistical significance (*p*-value) of glioma and metastasis. Significant values include decreased values of PME/Pi in the tumor group (1.22 ± 0.72) compared with controls (2.28 ± 1.44) with a *p*-value of 0.041. There is a significant decrease in PCr/Pi values (energy demand) in the tumor group (2.76 ± 0.73) compared with controls (4.13 ± 1.75) with a *p*-value of 0.050. Significant increase in Pi/ATP was noted in the tumor group (0.28 ± 0.09) compared with controls (0.22 ± 0.08) with a *p*-value of 0.049. Among the tumor group, PME/PCr values were significantly decreased in gliomas (0.35 ± 0.17) than metastasis (0.58 ± 0.23) compared with controls with a *p*-value of 0.047. A significant decrease in PME/ATP was noted in gliomas (0.25 ± 0.12) than metastasis (0.41 ± 0.14) compared with controls with a *p*-value of 0.034. The tumor group exhibits alkaline pH (7.12 ± 0.10) compared with the normal parenchyma (7.04 ± 0.06) with a significant *p*-value of 0.025. Glioma and metastasis could not be differentiated with pH. However, the perilesional edema of glioma shows alkaline pH (7.09 ± 0.06) and metastasis shows acidic pH (7.02 ± 0.05) with a significant *p*-value of 0.030 (►**Fig. 2**) mentioned in ►**Table 3**. We have also provided four illustrative cases from our sampled subjects, two cases of histopathologically proven Grade-2 (►**Fig. 3**)

Table 1 Mean integral values, standard deviation, and *p*-values of various phospholipid metabolites with ratios and statistical significance

Metabolites	Tumor	Periphery	Normal	*t*-Value	*p*-Value	Significance
PCr	660 ± 465	578 ± 469	663 ± 597	0.124	0.884	–
Pi	251 ± 178	179 ± 127	167 ± 99	1.609	0.212	–
PME	235 ± 84	297 ± 323	361 ± 392	0.678	0.513	–
PDE	228 ± 140	221 ± 198	205 ± 136	0.081	0.922	–
ATP	894 ± 548	851 ± 724	865 ± 758	0.016	0.984	–
PME/PDE	1.96 ± 2.33	1.90 ± 2.19	3.58 ± 5.04	1.126	0.334	–
PME/Pi	1.22 ± 0.72	1.74 ± 1.01	2.28 ± 1.44	3.468	0.041	+
PME/pCr	0.45 ± 0.22	0.49 ± 0.23	0.57 ± 0.24	1.17	0.320	–
PME/ATP	0.31 ± 0.14	0.34 ± 0.18	0.42 ± 0.17	1.708	0.194	–
PDE/Pi	1.06 ± 0.63	1.30 ± 0.57	1.44 ± 1.04	0.895	0.416	–
PDE/pCr	0.37 ± 0.20	0.40 ± 0.21	0.34 ± 0.20	0.318	0.730	–
PDE/ATP	0.26 ± 0.13	0.27 ± 0.11	0.26 ± 0.15	0.031	0.970	–
PCr/Pi	2.76 ± 0.73	3.59 ± 1.77	4.13 ± 1.75	3.23	0.050	+
PCr/ATP	0.73 ± 0.15	0.70 ± 0.14	0.78 ± 0.13	1.29	0.286	–
ATP/Pi	4.02 ± 1.87	5.07 ± 2.26	5.31 ± 2.35	1.504	0.234	–
Pi/ATP	0.28 ± 0.09	0.22 ± 0.06	0.19 ± 0.08	3.244	0.049	+
pH	7.12 ± 0.10	7.06 ± 0.07	7.04 ± 0.06	4.021	0.025	+

Abbreviations: ATP, adenosine triphosphate; PCr, phosphocreatine; PDE, phosphodiesters; pH, hydrogen ion concentration; Pi, inorganic phosphate; PME, phosphomonoesters.

Table 2 Mean, standard deviation, and *p*-value with various phospholipid ratios in glioma and metastasis with voxel of interest placed within the contrast-enhancing site of the lesion

Metabolites	Glioma		Metastasis		*p*-Value	Significance
	Lesion	Periphery	Lesion	Periphery		
PCr	777 ± 565	663 ± 623	484 ± 179	465 ± 52	0.247	–
Pi	298 ± 215	223 ± 151	181 ± 72	119 ± 50	0.227	–
PME	220 ± 84	324 ± 428	256 ± 85	262 ± 111	0.428	–
PDE	283 ± 135	288 ± 240	144 ± 106	132 ± 68	0.053	–
ATP	1,056 ± 666	1,028 ± 938	652 ± 119	614 ± 122	0.170	–
PME/PDE	0.96 ± 0.63	0.97 ± 0.55	3.45 ± 3.18	3.13 ± 2.98	0.114	–
PME/Pi	0.94 ± 0.50	1.18 ± 0.70	1.63 ± 0.86	2.49 ± 0.89	0.070	–
PME/pCr	0.35 ± 0.17	0.40 ± 0.20	0.58 ± 0.23	0.60 ± 0.25	0.047	+
PME/ATP	0.25 ± 0.12	0.26 ± 0.13	0.41 ± 0.14	0.46 ± 0.19	0.034	+
PDE/Pi	1.09 ± 0.43	1.29 ± 0.35	1.01 ± 0.90	1.32 ± 0.82	0.853	–
PDE/pCr	0.41 ± 0.15	0.49 ± 0.21	0.32 ± 0.26	0.28 ± 0.15	0.439	–
PDE/ATP	0.29 ± 0.11	0.30 ± 0.08	0.21 ± 0.16	0.23 ± 0.13	0.272	–
pCr/Pi	2.73 ± 0.76	2.86 ± 1.00	2.81 ± 0.75	4.57 ± 2.17	0.844	–
pCr/ATP	0.72 ± 0.07	0.64 ± 0.15	0.75 ± 0.22	0.77 ± 0.10	0.704	–
ATP/Pi	3.78 ± 0.97	4.37 ± 0.84	4.38 ± 2.83	6.01 ± 3.23	0.560	–
Pi/ATP	0.28 ± 0.06	0.24 ± 0.05	0.29 ± 0.13	0.19 ± 0.05	0.797	–

Abbreviations: ATP, adenosine triphosphate; PCr, phosphocreatine; PDE, phosphodiesters; Pi, inorganic phosphate; PME, phosphomonoesters.

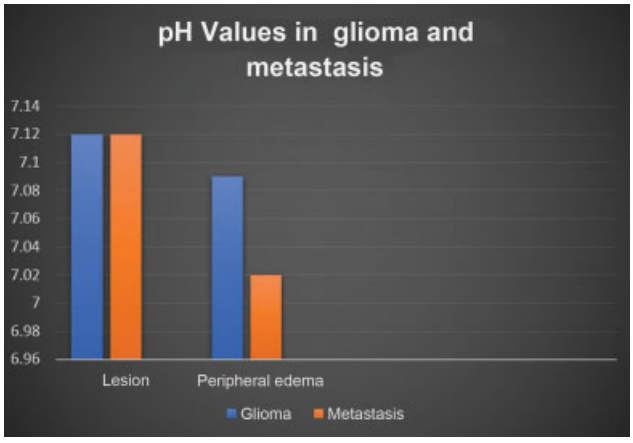

Fig. 2 Bar chart showing pH values of lesion and peripheral edema of glioma and metastases.

and Grade-4 (►**Fig. 4**) glioma followed by two cases of intraparenchymal cerebral metastases (►**Figs. 5** and **6**) with corresponding axial chemical shift image and spectroscopic values.

Discussion

It has been estimated that the incidence of central nervous system tumors in India was 5 to 10 cases per 100,000 people. The most common tumor was astrocytoma (38.7%), and 59.5% of all astrocytomas were high grade.[9] Gliomas and metastases were the most common intraparenchymal SOL and were commonly encountered in routine practice. Glioma and solitary metastasis pose a difficult diagnostic dilemma for conventional MRI, and a surgical biopsy might be required in such difficult situation.[10] Also, 30% of solitary metastasis might be the initial manifestation of a systemic cancer.[11] Differentiation between glioma and metastases is an important information required by the neurosurgeons to decide on curative surgical or palliative radiotherapy and for systemic workup, as the patient with metastasis might be benefitted rather than the patient with primary glioma. Conventional MRI sequences might not provide sufficient differentiation between these two. Advanced available methods for this differentiation currently are proton MRS, diffusion tensor imaging, diffusion-weighted imaging, and

Table 3 Mean, standard deviation, and *p*-value of biochemical pH value in glioma and metastasis in contrast-enhanced area and perilesional edema

pH	Glioma	Metastasis	*p*-Value	Significance
	Mean and SD	Mean and SD		
Lesion	7.12 ± 0.10	7.12 ± 0.12	0.821	–
Peripheral edema	7.09 ± 0.06	7.02 ± 0.05	0.03	+

Abbreviations: pH, hydrogen ion concentration; SD, standard deviation.

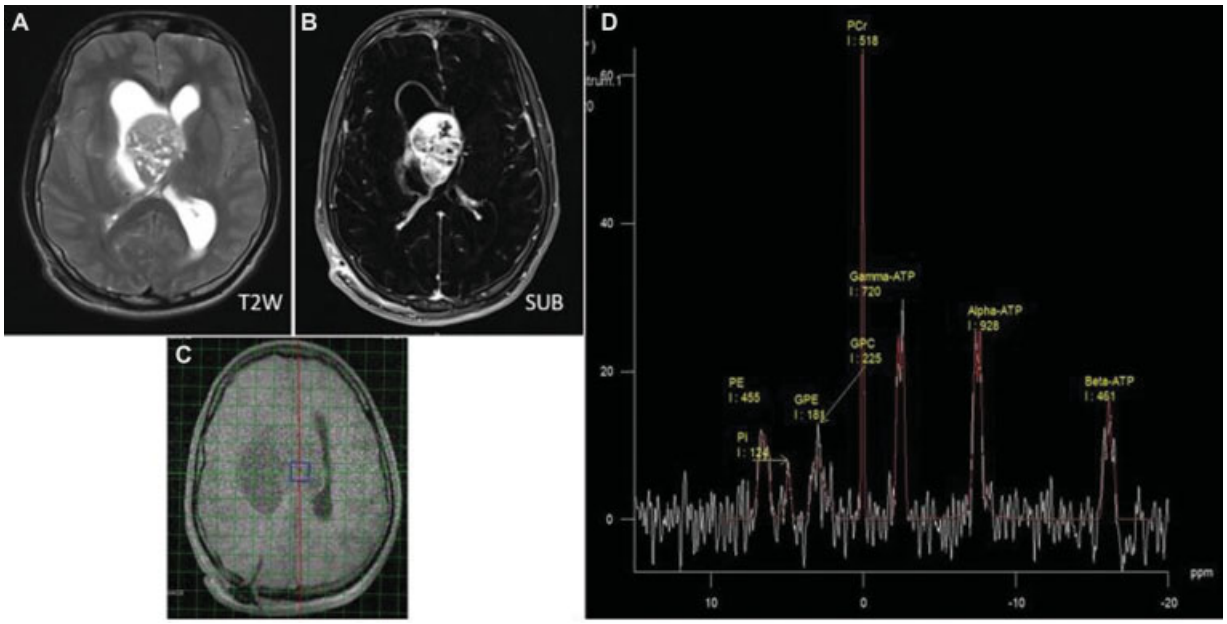

Fig. 3 (**A**) Axial T2-weighted images show mixed intense lesion noted in the body of corpus callosum (histopathologically proven Grade II glioma). (**B**) Postcontrast subtracted images show heterogeneous contrast enhancement. (**C** and **D**) Axial chemical shift imaging sequence of 31-phosphorus multinuclear spectroscopy and the spectroscopic integral values of various phospholipid metabolites.

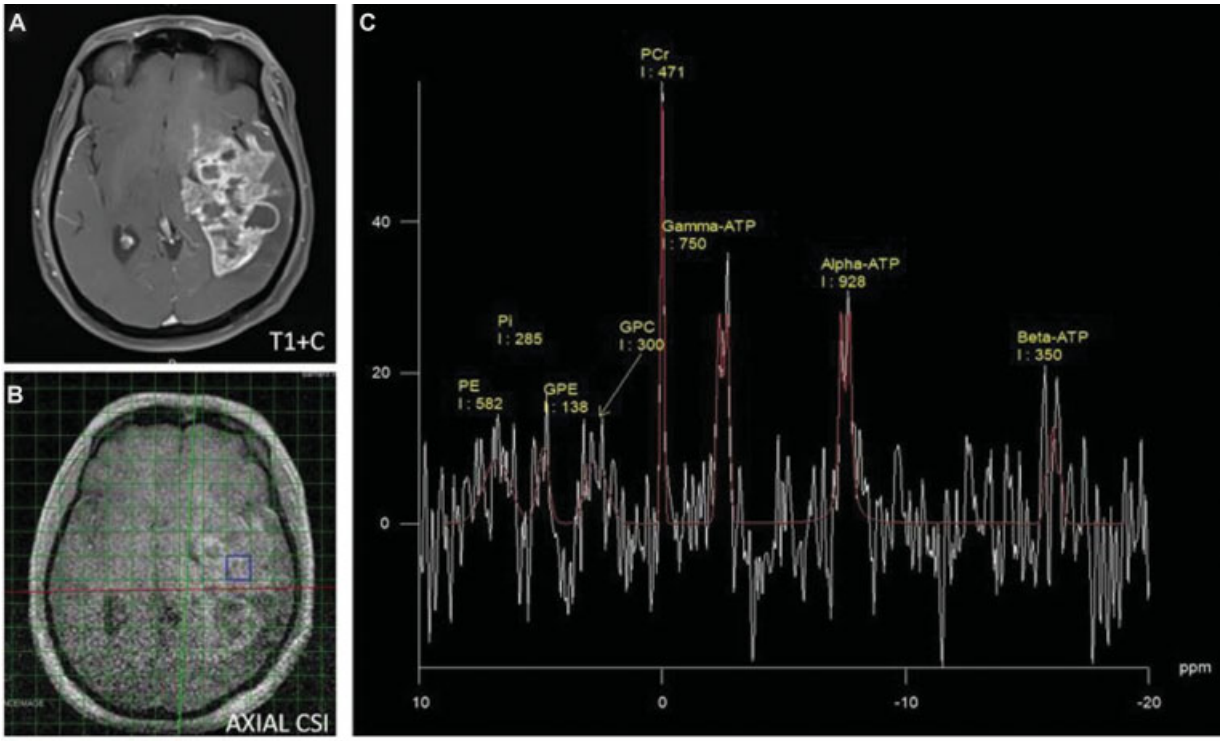

Fig. 4 (**A**) Postcontrast images show heterogeneous enhancing mass lesion in left temporal lobe (histopathologically proven Grade IV glioma). (**B** and **C**) Axial chemical shift imaging sequence of 31-phosphorus multinuclear spectroscopy and the spectroscopic integral values of various phospholipid metabolites.

dynamic susceptibility contrast-enhanced imaging.[12] 31-P MNS is a noncontrast imaging research tool that could be used for this purpose. Our study strives to evaluate the role of 31-P MNS in the differentiation of glioma from cerebral metastasis. The added advantage of 31-P MNS is that it allows the noninvasive method of evaluating the characterization of phosphate compounds and determination of the energy status within the tumor cells. The basic fundamental

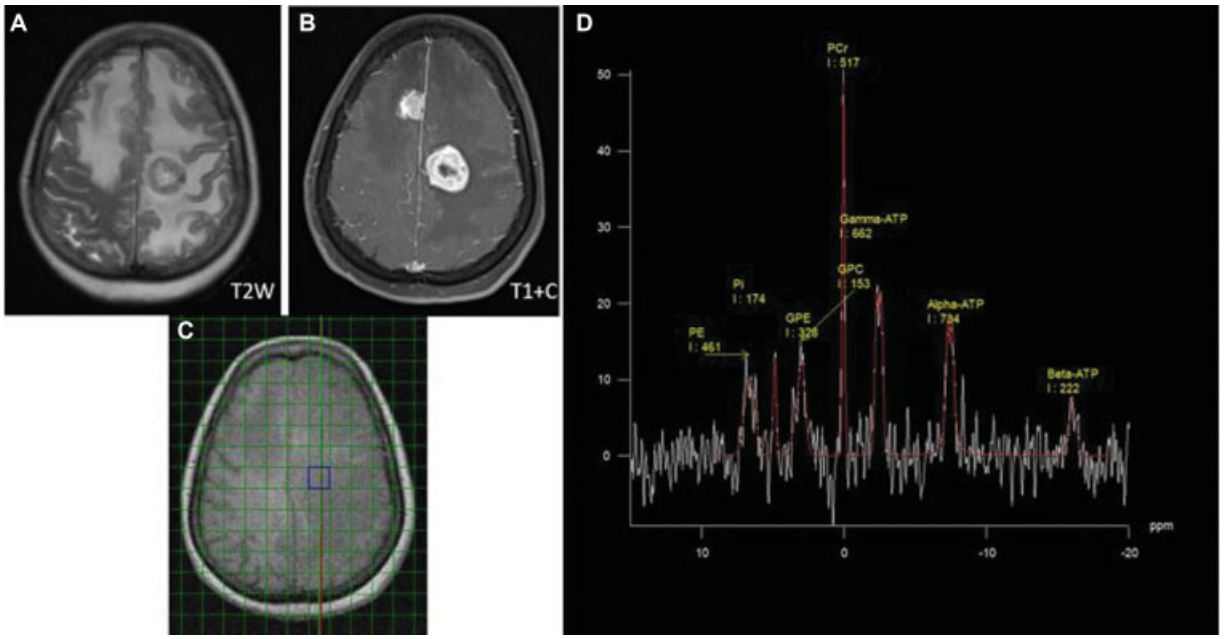

Fig. 5 (**A**) Axial T2-weighted images show multiple (two) mixed intensity lesion noted in bilateral high frontal region with surrounding disproportionate edema (cerebral metastasis/known case of Ca lung). (B) Postcontrast images show heterogeneous contrast enhancement. (**C** and **D**) Axial chemical shift imaging sequence of 31-phosphorus multinuclear spectroscopy and the spectroscopic integral values of various phospholipid metabolites.

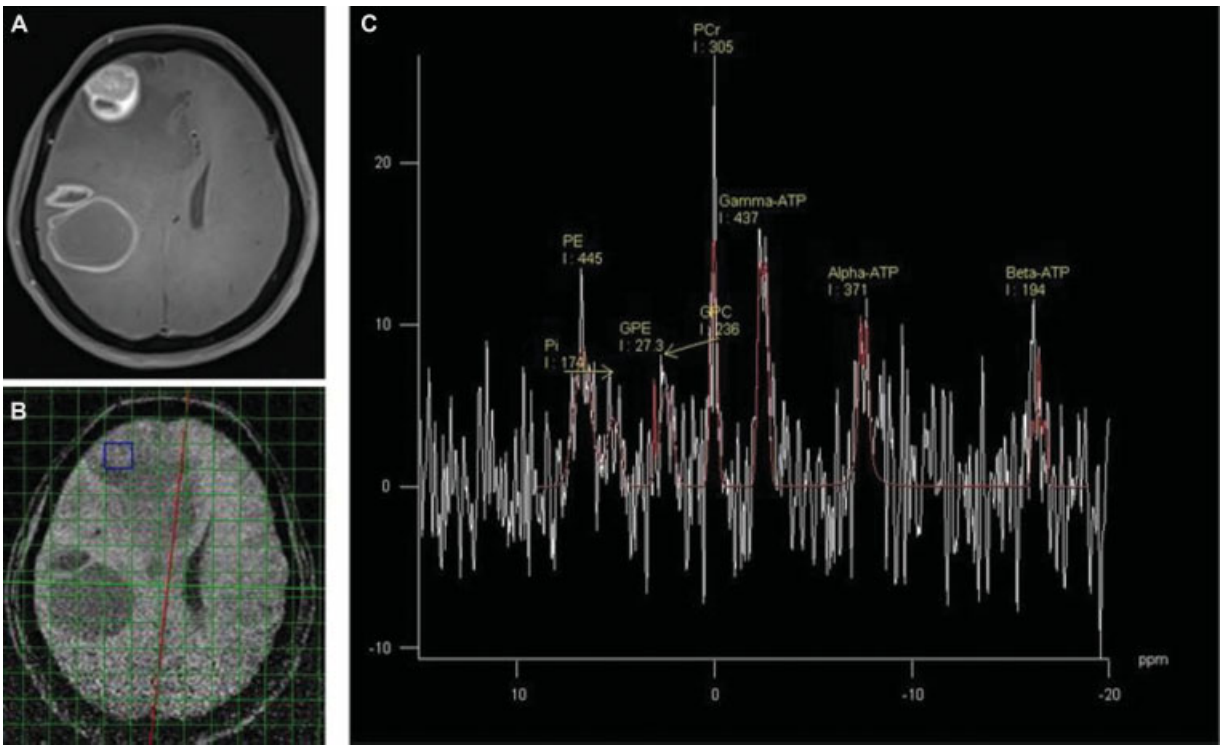

Fig. 6 (**A**) Axial postcontrast images show heterogeneous enhancing mass lesion in right frontal and parietal lobes (cerebral metastasis/known case of Ca lung). (**B** and **C**) Axial chemical shift imaging sequence of 31-phosphorus multinuclear spectroscopy and the spectroscopic integral values of various phospholipid metabolites.

processes of cells are bioenergetics, cell membrane phospholipid turnover, and intracellular pH,[13] and their relative in-vivo assessment could be possible by 31-P MNS.

The various metabolites that could be calculated were PME, PDE, PCr, Pi, and ATP, which are not absolute but just relative values[14] and multiple ratios can be then calculated and are as follows: PME/PDE, PME/Pi, PME/PCr, PME/ATP, PDE/Pi, PDE/PCr, PDE/ATP, PCr/Pi, PCr/ATP, ATP/Pi, and Pi/ATP. The major metabolites are PME (cytoplasmic membrane synthesis), PDE (cell wall structure), Pi (measure of free

energy liberated while hydrolysis of ATP), and PCr (represents PCr).[15]

The main components of PME were phosphocholine and phosphoethanolamine.[15] PME integral values represent membrane synthesis, membrane turnover, or rapid cell growth, and decrease in PME values noted in gliomas compared with abscess.[16] Our study showed a decrease in PME integral values in both glioma and metastasis compared with normal brain parenchyma, signifying increased membrane synthesis in both of these tumors, but statistical significance could not be proved between glioma (220 ± 84) and metastasis (256 ± 85) as both of the tumors show increased cell turnover.

PDE values include glycerol-3-phosphoethanolamine and glycerol-3-phosphocholine. This contributes to the cell wall structure, and increased values signify the presence of breakdown products of metabolism due to high energy demand in glioma and metastasis. Previous studies by Arnold et al and Heindel et al showed decreased PDE values in high-grade gliomas and metastasis.[16,17] Our study showed increased PDE values in gliomas (283 ± 135) and decreased PDE values in metastasis (144 ± 106) compared with the normal brain parenchyma (205 ± 136). A high PME/PDE ratio was found in astrocytoma, metastasis, and lymphoma compared with the controls.[18] Our study showed no significant increase in the values of PME/PDE among gliomas (0.96 ± 0.63) and metastasis (3.45 ± 3.18).

Besides oxidative phosphorylation that occurs in the cells for energy metabolism, creatine kinase was also involved in cellular metabolism to maintain homeostasis. It acts as an energy reservoir by transferring the energy through the exchange of phosphorus with the ADP in the production of ATP by the following reaction:[19]

$$\boldsymbol{ADP + PCr + H^{+} \leftrightarrow ATP + PCr}$$

In gliomas and metastasis, owing to the high energy demand and increased cellular metabolism, there will be decreased PCr and increased ATP integral values. Thus, this relationship between PCr and ATP can be represented by the PCr/ATP ratio. We found a decreased value of PCr/ATP ratio in gliomas (0.72 ± 0.07) and metastasis (0.75 ± 0.22) compared with normal (0.78 ± 0.13) parenchyma but no statistical difference was made out (p-value: 0.704) between glioma and metastases. PCr/Pi ratio represents the energy demand of the cells and a significant decrease in PCr/Pi ratio was reported in metastasis by Cady et al[13] due to increased necrosis and hypoxia in metastasis. Our study showed decreased PCr/Pi ratio in both gliomas and metastasis (2.76 ± 0.73) compared with normal parenchyma (4.13 ± 1.75) with a significant p-value of 0.050 as both of the lesions show high energy demand compared with the normal brain parenchymal cells and these cells would obtain ATP from PCr. However, statistical difference between glioma (2.73 ± 0.76) and metastasis (2.81 ± 0.75) could not be made out (p-value: 0.844).

Ha et al in their study reported that PME/PCr ratio was significantly lower in lymphoma as compared with astrocytoma and decreased in astrocytoma compared with controls, but statistical significance was not proven.[18] Our study reported the statistical significance of low PME/PCr in glioma (0.35 ± 0.17) compared with normal parenchyma (0.57 ± 0.24) and significantly lower compared with metastasis (0.58 ± 0.23) with a p-value of 0.047. This low PME/PCr ratio can be correlated with elevated PCr in gliomas and lymphomas.[18] The ratio of PME/ATP showed no significance between glioma and metastasis in the study of Ha et al.[18] Our study showed a significant decrease in PME/ATP in gliomas (0.25 ± 0.12) compared with normal parenchyma (0.42 ± 0.17) with a p-value of 0.039, but no significant change was noted in metastasis (0.41 ± 0.14).

Free intracellular Pi produced from the hydrolysis of ATP to ADP and Pi would liberate a large amount of free energy.[20] Significant high levels of Pi in gliomas and metastasis were due to the presence of hypoxia and consumption of ATP to liberate ADP and Pi. Our study showed increased Pi values in gliomas (298 ± 215) and metastasis (181 ± 72) compared with the normal parenchyma (167 ± 99), but no statistical difference was made out between the two (p-value: 0.227).

The pH of tumors may be acidic or alkaline depending on the level of oxygenation. The technical difficulty of separation of Pi and PCr resonances might hinder the accurate estimation of pH in tumors.[21] Microelectrode measurements demonstrate extracellular pH (pHe) values ranging from 6.5 to 6.9 for intraparenchymal tumors and values of 7.0 to 7.5 for normal cells.[22] In spite of their increased H1 production and acidic extracellular milieu, 31-P NMR spectroscopic studies of gliomas have reported that the intracellular pH (pHi) measured in situ is more alkaline (pH 7.12–7.24) than that of normal brain (pH 6.99–7.05).[23] Our study showed statistically significantly increased pH in glioma (7.12 ± 0.10) and metastasis (7.12 ± 0.12) compared with normal parenchyma (7.04 ± 0.06) with a p-value of 0.025. Maintenance of an alkaline pH has been shown to be necessary for various mechanisms involved in cellular proliferation because several intracellular metabolic enzymes have alkaline pH optima. One such enzyme called phosphofructokinase requires optimal pH of 7.2 and decrease in pH would lead to decreased activity of the enzyme.[24] Even though glioma and metastasis showed a relative increase in pH values, they could not be differentiated based on the lesional pH values. The calculated pH values in gliomas correlate with previous study of Ha et al.[18] However, the pH values of metastases in our study did not correlate with previous study. The perilesional edema would be helpful where the pH of perilesional edema of glioma (7.09 ± 0.06) was higher than that of metastasis (7.02 ± 0.05) with a p-value of 0.030. This might be due to the permeative pattern of mass lesion in gliomas with malignant cells noted in perilesional edema, but metastasis tends to be more encapsulated with no malignant cells in the perilesional edema.[25,26] Maintz et al in their study reported alkalinization of brain tumors with gliomas showing a pH of 7.12 ± 0.02.[27] This alkalinization was contrary to the assumption that tumor cells have acidotic metabolism due to the conversion of pyruvate to lactic acid as a result of glycolysis. Okada et al in their study by inducing gliomas

in cats showed solid part of the tumor was alkaline and the necrotic part was acidic and stated that the voxel of interest placed on a portion of the tumor might contain solid and necrotic components and thus measurement might be inaccurate.[28] But in our study, we placed the voxel of interest after assessing the tumor morphology in contrast sequences to avoid placing the voxel in necrotic areas. The alkalinization might be due to the acceleration of the Na^+/H^+ exchange due to catabolites in proliferating cells, which leads to an increase in pH value.[29] Thus, our study helps in differentiating the glioma and metastases by calculating the pH values of the perilesional edema.

Limitations

31-P MNS is an advanced in vivo, noninvasive MRI tool to quantify the various phospholipid metabolites but till now not accepted in the routine diagnostic tool. This is because a specially designed and dedicated radiofrequency coil system is required to obtain a satisfactory 31-P MNS spectrum, which is not only expensive but also requires higher magnetic strengths. However, due to the short relaxation time of 31-P metabolites, the routinely used in-built scanner sequences like stimulated echo acquisition mode and point-resolved spectroscopy are not used to obtain the spectrum and it is recommended to apply rare techniques like image-selected in-vivo spectroscopy or pulse acquire techniques.[30] Other limitations include the difficulty in decoupling the double, triple, and quadruple peak spectral waveforms of various 31-P metabolites, low signal-to-noise ratio, and insufficient temporal resolution in the widely available magnetic resonance (MR) scanners (<3T).[31] Thus, to obtain a satisfactory 31-P MNS spectrum, a specially dedicated radiofrequency coil, sequence, and higher field magnet of at least 3T are needed. Voxel bleeding effect due to point spread function is a major limitation of MNS due to contamination of the large voxel size from other tissues like large necrotic areas, cerebrospinal fluid, and bone. We tried to place voxels so as to avoid these areas wherever possible.

Conclusion

Advanced MR techniques like dynamic susceptibility-weighted contrast perfusion and MRS are established and help in preoperative differentiation of glioma and metastases. However, 31-P MNS helps to provide new insight into the cellular constituents and pH of gliomas and metastases that are not possible with the former. The phospholipid ratios of PME/PCr and PME/ATP were significantly decreased in the glioma compared with metastases. Though the pH value of glioma and metastases could not differentiate these two entities, the pH of peritumoral edema helps in differentiating them. Thus, our results were significant in differentiation between these two. However, due to the additional high expense, it is available as a research tool in very few institutions in India and very few studies are available focusing on this unique advanced research tool that helps to assess the energy characteristics of brain tumors.

Funding
None.

Conflict of Interest
None.

References

1 Mirkes C, Shajan G, Chadzynski G, Buckenmaier K, Bender B, Scheffler K. (31)P CSI of the human brain in healthy subjects and tumor patients at 9.4 T with a three-layered multi-nuclear coil: initial results. MAGMA 2016;29(03):579–589
2 Lei H, Zhu XH, Zhang XL, Ugurbil K, Chen W. In vivo 31P magnetic resonance spectroscopy of human brain at 7 T: an initial experience. Magn Reson Med 2003;49(02):199–205
3 Ren J, Sherry AD, Malloy CR. (31)P-MRS of healthy human brain: ATP synthesis, metabolite concentrations, pH, and T1 relaxation times. NMR Biomed 2015;28(11):1455–1462
4 Bonora M, Patergnani S, Rimessi A, et al. ATP synthesis and storage. Purinergic Signal 2012;8(03):343–357
5 Verma A, Kumar I, Verma N, Aggarwal P, Ojha R. Magnetic resonance spectroscopy - revisiting the biochemical and molecular milieu of brain tumors. BBA Clin 2016;5:170–178
6 Morrison EA, Robinson AE, Liu Y, Henzler-Wildman KA. Asymmetric protonation of EmrE. J Gen Physiol 2015;146(06):445–461
7 Hattingen E, Magerkurth J, Pilatus U, et al. Phosphorus and proton magnetic resonance spectroscopy demonstrates mitochondrial dysfunction in early and advanced Parkinson's disease. Brain 2009;132(Pt 12):3285–3297
8 Cichocka M, Kozub J, Urbanik A. PH measurements of the brain using phosphorus magnetic resonance spectroscopy ((31)PMRS) in healthy men - comparison of two analysis methods. Pol J Radiol 2015;80:509–514
9 Dasgupta A, Gupta T, Jalali R. Indian data on central nervous tumors: a summary of published work. South Asian J Cancer 2016;5(03):147–153
10 Davis FG, McCarthy BJ, Berger MS. Centralized databases available for describing primary brain tumor incidence, survival, and treatment: Central Brain Tumor Registry of the United States; Surveillance, Epidemiology, and End Results; and National Cancer Data Base. Neuro-oncol 1999;1(03):205–211
11 Schiff D. Single brain metastasis. Curr Treat Options Neurol 2001; 3(01):89–99
12 Hollingworth W, Medina LS, Lenkinski RE, et al. A systematic literature review of magnetic resonance spectroscopy for the characterization of brain tumors. AJNR Am J Neuroradiol 2006; 27(07):1404–1411
13 Cady EB, Hennig J, Martin E. Magnetic Resonance Spectroscopy in Imaging of the Central Nervous System of Neonates. New York: Springer Verlag
14 Maintz D, Heindel W, Kugel H, Jaeger R, Lackner KJ. Phosphorus-31 MR spectroscopy of normal adult human brain and brain tumours. NMR Biomed 2002;15(01):18–27
15 Kamble RB, Peruvumba N J, Shivashankar R. Energy status and metabolism in intracranial space occupying lesions: a prospective 31p spectroscopic study. J Clin Diagn Res 2014;8(11):RC05–RC08
16 Arnold DL, Emrich JF, Shoubridge EA, Villemure JG, Feindel W. Characterization of astrocytomas, meningiomas, and pituitary adenomas by phosphorus magnetic resonance spectroscopy. J Neurosurg 1991;74(03):447–453
17 Heindel W, Bunke J, Glathe S, Steinbrich W, Mollevanger L. Combined 1H-MR imaging and localized 31P-spectroscopy of intracranial tumors in 43 patients. J Comput Assist Tomogr 1988;12(06):907–916
18 Ha DH, Choi S, Oh JY, Yoon SK, Kang MJ, Kim KU. Application of 31P MR spectroscopy to the brain tumors. Korean J Radiol 2013;14 (03):477–486

19 Liu Y, Gu Y, Yu X. Assessing tissue metabolism by phosphorous-31 magnetic resonance spectroscopy and imaging: a methodology review. Quant Imaging Med Surg 2017;7(06):707–726
20 Steen RG. Characterization of tumor hypoxia by 31P MR spectroscopy. AJR Am J Roentgenol 1991;157(02):243–248
21 Kopp SJ, Krieglstein J, Freidank A, Rachman A, Seibert A, Cohen MM. P-31 nuclear magnetic resonance analysis of brain: II. Effects of oxygen deprivation on isolated perfused and nonperfused rat brain. J Neurochem 1984;43(06):1716–1731
22 Vaupel P, Kallinowski F, Okunieff P. Blood flow, oxygen and nutrient supply, and metabolic microenvironment of human tumors: a review. Cancer Res 1989;49(23):6449–6465
23 Hubesch B, Sappey-Marinier D, Roth K, Meyerhoff DJ, Matson GB, Weiner MW. P-31 MR spectroscopy of normal human brain and brain tumors. Radiology 1990;174(02):401–409
24 Horská A, Barker PB. Imaging of brain tumors: MR spectroscopy and metabolic imaging. Neuroimaging Clin N Am 2010;20(03): 293–310
25 Wike-Hooley JL, Haveman J, Reinhold HS. The relevance of tumour pH to the treatment of malignant disease. Radiother Oncol 1984;2(04):343–366
26 Kerschbaumer J, Pinggera D, Steiger R, et al. Results of phosphorus magnetic resonance spectroscopy for brain metastases correlate with histopathologic results. World Neurosurg 2019;127: e172–e178
27 Maintz D, Heindel W, Kugel H, Jaeger R, Lackner KJ. Phosphorus-31 MR spectroscopy of normal adult human brain and brain tumours. NMR Biomed 2002;15(01):18–27
28 Okada Y, Kloiber O, Hossmann KA. Regional metabolism in experimental brain tumors in cats: relationship with acid/base, water, and electrolyte homeostasis. J Neurosurg 1992;77(06): 917–926
29 Oberhaensli RD, Hilton-Jones D, Bore PJ, Hands LJ, Rampling RP, Radda GK. Biochemical investigation of human tumours in vivo with phosphorus-31 magnetic resonance spectroscopy. Lancet 1986;2(8497):8–11
30 Buonocore MH, Maddock RJ. Magnetic resonance spectroscopy of the brain: a review of physical principles and technical methods. Rev Neurosci 2015;26(06):609–632
31 Andrade CS, Otaduy CG, Park EJ, Leite CC. Phosphorus-31 MR spectroscopy of the human brain: technical aspects and biomedical applications. Int J Curr Res Rev. 2014;6:41–57

